ChemComm

Accepted Manuscript

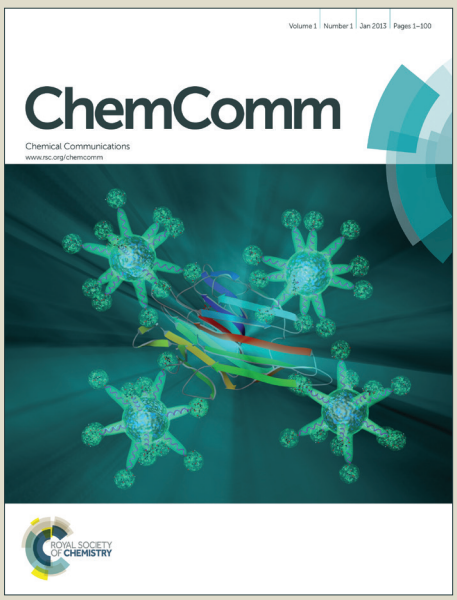

ROYAL SOCIETY OF CHEMISTRY

www.rsc.org/chemcomm

ChemComm

RSCPublishing

COMMUNICATION

Highly efficient deep-blue phosphorescence from heptafluoropropyl-substituted iridium complexes

Cite this: DOI: 10.1039/xoxxoooooox

Jung-Bum Kim,‡[a] Seung-Hoon Han,‡[b] Kiyull Yang,[d] Soon-Ki Kwon,*[c] Jang-Joo Kim,*[a] and Yun-Hi Kim*[b]

Received ooth January 2012,
Accepted ooth January 2012

DOI: 10.1039/xoxxoooooox

www.rsc.org/chemcomm

New deep-blue iridium complexes, consisting of a heptafluoropropyl (HFP) substituent at 3' position of 2',4''-difluororphenyl, which has deep HOMO level and decreased shoulder electronic transition and inhibit self-quenching due to sterically hindered group without conjugation. OLED using $(HFP)_2Ir(mpic)$ exhibited maximum EQE of 21.4 % with CIE of (0.146, 0.165).

Red and green phosphorescent iridium complexes are used in organic light emitting didoes (OLEDs) for displays and solid state lighting systems. Recently, external quantum efficiencies (EQEs) of over 30% have been reported.[1-5] However, development of highly efficient blue, especially deep blue emitting phosphorescent dyes still remains as a challenge for high performance full color displays and high quality white OLEDs. Iridium(III)bis[(4,6-difluorophenyl)-pyridinato-N,C2′] picolinate (FIrpic) has been widely used as a dopant material for sky blue PHOLEDs with high external quantum efficiency.[6-14] However, it is difficult to synthesize deep blue phosphorescent materials that exhibit high color purity as well as high photoluminescence quantum yields (PLQYs).[15-17] Recently, a couple of strategies have been developed for deep-blue emitting iridium complexes. One strategy involves controlling the energy levels of the highest occupied molecular orbital (HOMO) and the lowest unoccupied molecular orbital (LUMO) localized primarily on the phenyl and pyridyl moieties, respectively, of the cyclometalated ligands.[20] The electron-withdrawing group in the phenyl part lowers the HOMO level while the electron-donating group in the pyridyl part increases the LUMO level. We had previously reported that the position of the substituent in dimethylated iridium complexes affects the color purity and efficiency of the corresponding OLEDs.[21] We also recently reported that overly strong electron-withdrawing groups such as heptafluorocarbonyl unit decreased both HOMO and LUMO level.[22] Therefore, appropriately strong electron-withdrawing groups are required to effectively decrease the HOMO level without lowering the LUMO level. A second strategy is to control the vibration shoulder intensities to have larger emission oscillator strength at the shortest wavelength than the oscillator strength of other longer wavelength shoulder peaks. Since most of blue-emitting iridium complexes have vibrational shoulder peaks at longer wavelength, larger oscillator strengths of the longer wavelength shoulder peaks have an effect of diminishing the color purity for deep blue.

In this article, we report three new deep-blue iridium complexes, which consist of a heptafluoropropyl (HFP) substituent at the 3' position of 2',4''-difluororphenyl as the main ligand and a picolinate with 3-methylpyridine (mpic) or a trifluoromethylated triazole (fptz) as the ancillary ligands. HFP was selected as an electron-withdrawing group that does not exhibit extended π-conjugation and a methyl group at the 4 position of the pyridine group. Perfluoro alkyl groups have several effects in Ir(III) cyclometalated complexes. One is an appropriate electron-withdrawing effect without conjugation on the ligand π-system. The density functional theory (DFT) calculation showed that heptafluoro alkyl group more strongly affects the HOMO level than LUMO level, resulting in large band gap and small oscillator strength of long wavelength vibrational shoulder peaks leading to deep-blue emission. Another effect is to provide steric hindrance around the metal to increase the PLQY.[23] In addition, fluorinated substituents in the aromatic ligands of metal complexes makes it highly volatile, enabling facile, high-yielding purification by sublimation a feature beneficial for the mass were used in high-efficiency, deep blue phosphorescent OLEDs; however, the color purity was rather limited.[18-19]

[a]*Department of Materials Science and Engineering and the Center for Organic Light Emitting Diodes, Seoul National University, Seoul 151-742, South Korea, E-mail: jjkim@snu.ac.kr*
[b]*Department of Chemistry and ERI, Gyeongsang National University, Jinju 66-701, South Korea, E-mail: ykim@gnu.ac.kr*
[c]*School of Materials Science and Engineering and ERI, Gyeongsang National University, Jinju 66-701, South Korea, E-mail: skwon@gnu.ac.kr*
[d]*Department of Chemistry Education, Gyeongsang National University, Jinju 660-701, South Korea*

†Electronic supplementary information (ESI) available: Experimental details, CV, TGA and DFT calculations.

‡Jung-Bum Kim and Seung-Hoon Han contributed equally.

production of displays. A trifluoromethyl-substituted triazole or a picolinate ancillary ligand is also utilized so that C-linked 2-pyridyl-azoles can form a stable chelate using two proxymal nitrogen atoms. In addition, trifluoromethyl-substituted triazoles are strongly acidic; a feature reinforced by the incorporation of the electron-withdrawing heptafluoropropyl substituent.[24]

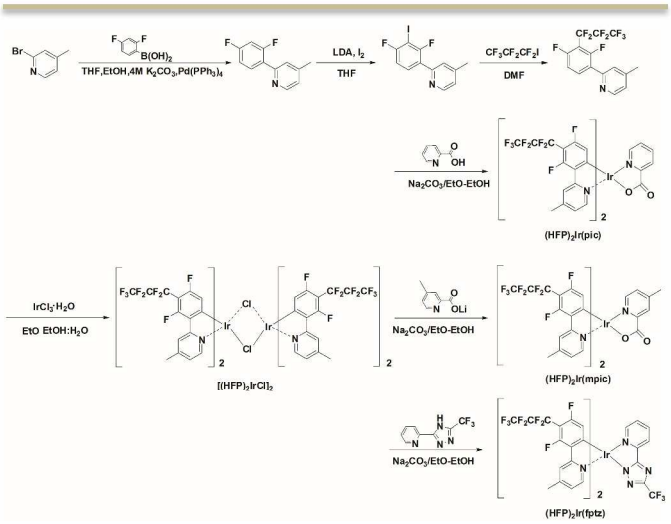

Figure 1. Synthetic schemes of the Iridium complexes.

Figure 1 illustrates the synthesis of heptafluoropropyl substituted ligand and iridium complexes. The ligand, 2-(2,4-difluoro-3-(perfluoropropyl)phenyl)-4-methylpyridine, was obtained by Ulmann coupling of heptafluoropropyl iodide and 2-(2,4-difluoro-3-iodophenyl)-4-methylpyridine. 2-(2,4-Difluorophenyl)-4-methylpyridine was synthesized using iodine and under lithium diisopropylamide (LDA) base condition. The cyclometalated iridium μ-chloro-bridged dimer was prepared by the reaction of ligand and $IrCl_3•H_2O$ in a mixture of 2-ethoxyethanol and water by the well-known Nonoyama reaction. The new iridium complexes were prepared by reacting the chloro-bridged dimer with the ancillary ligands in the 2-ethoxyethanol with sodium bicarbonate. The new iridium complexes, $(HFP)_2Ir(pic)$, $(HFP)_2Ir(mpic)$, and $(HFP)_2Ir(fptz)$, were characterized by ^{1}H-NMR and ^{19}F-NMR spectroscopy and high-resolution mass spectrometry (HRMS). (Synthesis details in supporting information)

DFT calculations of the iridium complexes were carried out by optimizing the geometries of the molecules using the B3LYP/6-31G basis set for the ligands, and the relativistic effective core potential of Los Alamos and Double- basis sets (LANL2DZ)[25] for Ir (as implemented in Gaussian 03 package[22]). Time-dependent-DFT (TD-DFT)[26] calculations were also performed to estimate the energy levels, orbital electron density distributions and singlet and triplet transition energies on the basis of the structures optimized in their ground states. The HOMO, HOMO-1, LUMO, and LUMO+1 for $(HFP)_2Ir(pic)$, $(HFP)_2Ir(mpic)$, and $(HFP)_2Ir(fptz)$ are shown Figure S1. The HOMO levels of $(HFP)_2Ir(pic)$, $(HFP)_2Ir(mpic)$, and $(HFP)_2Ir(fptz)$ were mostly distributed over the phenyl ring of the main ligand, with a large contribution from the d atomic orbital and a slight contribution from the ancillary ligand. For comparison, we calculated the HOMO and LUMO levels of $(TFM)_2Ir(pic)$, $(TFM)_2Ir(mpic)$, and $(TFM)_2Ir(fptz)$ with already reported trifluormethyl group.[27] The HOMO levels of $(HFP)_2Ir(pic)$, $(HFP)_2Ir(mpic)$, and $(HFP)_2Ir(fptz)$ with strongly electron withdrawing heptafluoropropyl group were calculated as -6.22, -6.17, and -6.49 eV, respectively, while the HOMO levels of $(TFM)_2Ir(pic)$, $(TFM)_2Ir(mpic)$, and $(TFM)_2Ir(fptz)$ with the trifluormethyl group were calculated to be -6.17, -6.12, and -6.45 eV, respectively. (See supporting information, Figure S1, Table S3-6) These results suggest that the introduction of strongly electron-withdrawing heptafluoropropyl groups lowers the HOMO levels. The LUMO orbitals of the complexes were mostly distributed over one of the main ligands and the ancillary ligand. The LUMO levels of $(HFP)_2Ir(pic)$, $(HFP)_2Ir(mpic)$, and $(HFP)_2Ir(fptz)$ with strongly electron withdrawing heptafluoropropyl group were calculated as -2.35, -2.25, and -2.46 eV, respectively, while those of $(TFM)_2Ir(pic)$, $(TFM)_2Ir(mpic)$, and $(TFM)_2Ir(fptz)$ with trifluormethyl group were calculated to be -2.33, -2.23, and -2.43 eV, respectively. Compared with the trifluoromethyl group, the strongly electron-withdrawing heptafluoropropyl group has a greater effect on the HOMO level than it does on the LUMO level. In addition, compared to the picolinate ancillary ligand, the strongly electron-withdrawing triazole ancillary ligand decreased the HOMO level while the electron-donating methylated picolinate ancillary ligand increased the LUMO level. As a result, the band gaps increase in the following order: $(HFP)_2Ir(pic)$ < $(HFP)_2Ir(mpic)$ < $(HFP)_2Ir(fptz)$. Moreover, the band gaps are larger than those of $(TFM)_2Ir(pic)$, $(TFM)_2Ir(mpic)$, and $(TFM)_2Ir(fptz)$, each of which contains the trifleoromethyl group. Recently, we reported that the strong heptafluorocarbonyl substituted iridium complexes, $(HF)_2Ir(pic)$ and $(HF)_2Ir(fptz)$ lowered the LUMO levels more than trifluorocarbonyl substituted iridium complexes, $(TF)_2Ir(pic)$ and $(TF)_2Ir(fptz)$, increasing the band gaps in the following order: $(HF)_2Ir(pic)$ < $(TF)_2Ir(pic)$ < $(HF)_2Ir(fptz)$ < $(TF)_2Ir(fptz)$.[27] These results suggest that the strongly electron-withdrawing heptafluoropropyl group is an effective substitent for acessing the deepest blue emission.

Cyclic voltammetry (CV) was used to measure the HOMO levels of the iridium complexes (Figure S2). The HOMO levels of $(HFP)_2Ir(pic)$, $(HFP)_2Ir(mpic)$, and $(HFP)_2Ir(fptz)$ were found to be -5.94, -5.92, and -6.13 eV, respectively. The HOMO levels are in the same order as the DFT calculation. The LUMO levels were obtained from the optical band gaps and the HOMO levels. The HOMO and LUMO levels and the optical band gaps are summarized in Table S1.

Thermal properties were evaluated by thermogravimetric analysis (TGA) and differential scanning calorimetry (DSC) under a nitrogen

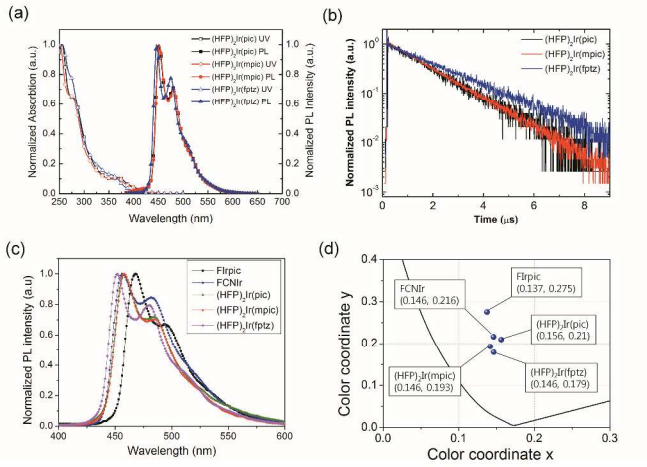

Figure 2. (a) UV−vis absorption and PL spectra of the iridium complexes in $CHCl_3$. (b) transient PL spectra of mCPPO1 films doped with the iridium complexes in the amount of 10 wt %. (c) PL spectra of mCPPO1 films doped with 10 wt% Firpic, FCNIr, $(HFP)_2Ir(pic)$, $(HFP)_2Ir(mpic)$, and $(HFP)_2Ir(fptz)$. (d) (CIE) coordinates calculated from PL spectra of Firpic, FCNIr, $(HFP)_2Ir(pic)$, $(HFP)_2Ir(mpic)$, and $(HFP)_2Ir(fptz)$.

atmosphere. The 5% weight loss temperatures of the iridium complexes were 366 °C for $(HFP)_2Ir(pic)$, 368 °C $(HFP)_2Ir(mpic)$, and 355 °C for $(HFP)_2Ir(fptz)$. Glass transition was not observed up to 250 °C. These results suggest that the new iridium complexes have good thermal stability (Figure S3, Table S7).

Figure 2 (a) shows the ultraviolet-visible (UV-vis) absorption and PL spectra of the iridium complexes in a $CHCl_3$ solution (10^{-5} M) at room temperature. Each of the complexes, $(HFP)_2Ir(pic)$, $(HFP)_2Ir(mpic)$, and $(HFP)_2Ir(fptz)$, displayed strong absorption bands around 255 nm, which can be attributed to intraligand π-π* transitions. The absorption bands at 277 nm for $(HFP)_2Ir(pic)$, 278 nm for $(HFP)_2Ir(mpic)$ and 272 nm for $(HFP)_2Ir(fptz)$ represent the spin-allowed ^{1}π-π* transition (ligand-centered absorptions). The absorptions shown at 370 nm for $(HFP)_2Ir(pic)$, 372 nm for $(HFP)_2Ir(mpic)$, and 356 nm for $(HFP)_2Ir(fptz)$ can be assigned to the singlet metal to ligand charge-transfer (^{1}MLCT) transitions. The spin-forbidden triplet ^{3}MLCT or ^{3}LC transitions (or both) appeared as low-energy absorption shoulders at approximately 410 nm for the complexe with the trifluoromethyl-substituted triazole and 420 nm for the complexes with the picolinate and the methylpicolinate ancillary ligand, respectively. The absorption maximum of the iridium complex with the methyl picolinate ancillary ligand was similar to that with picolinate ancillary ligand, while the absorption maxima of the iridium complex with the trifluoromethyl-substituted triazole ancillary ligand was blue shifted by approximated 10 nm. The complexes, $(HFP)_2Ir(pic)$, $(HFP)_2Ir(mpic)$, and $(HFP)_2Ir(fptz)$ showed intensely blue phosphorescence in $CHCl_3$ solution at room temperature, with the emission peaks at 451 and 479 nm for $(HFP)_2Ir(pic)$, 452 and 480 nm for $(HFP)_2Ir(mpic)$, and 446 and 475 nm for $(HFP)_2Ir(fptz)$.

The PLQYs of the iridium complexes were measured using 9-(3-(9H-carbazole-9-yl)phenyl)-3-(dibromophenylphosphoryl)-9H-carbazole (mCPPO1) films doped with 10 wt% of the iridium complexes. An integrating sphere was used for the measurements. The PLQYs of $(HFP)_2Ir(pic)$, $(HFP)_2Ir(mpic)$, and $(HFP)_2Ir(fptz)$ were determined to be 81 ± 3%, 90 ± 3% , and 53 ± 3%, respectively. The heptafluoropropyl substitutents with bulky ancillary ligand within the iridium complexes enhanced the steric hindrance of molecules to suppress the self-quenching due to reduction of bimolecular interactions, increasing the PLQYs.[22,23]

The transient PL of the doped films is shown in Figure 2 (b). The exciton lifetimes of the iridium complexes were 1.46, 1.47, and 1.99 for $(HFP)_2Ir(pic)$, $(HFP)_2Ir(mpic)$, and $(HFP)_2Ir(fptz)$, respectively. The iridium complexes with the picolinate-based ancillary ligand shows relatively shorter lifetimes than does the iridium(III) complex with the trifluoromethyl-substituted triazole ligand.

Figure 2 (c) shows shows the normalized PL spectra of mCPPO1 films doped with 10 wt% Firpic, FCNIr, $(HFP)_2Ir(pic)$, $(HFP)_2Ir(mpic)$, and $(HFP)_2Ir(fptz)$. It is interesting to note that $(HFP)_2Ir(pic)$ and $(HFP)_2Ir(mpic)$ showed the lowest intensity of the 0−1 vibronic transitions among the complexes, resulting in the deepest blue Commission Internationale de l'Eclairage (CIE) coordinates calculated from the PL spectra of blue emitters. The color properties of materials are illustrated in Figure 2 (d), which shows that our iridium complexes have the deepest CIE coordinates.

Phosphorescent blue OLEDs were fabricated using the iridium complexes as dopants within a phosphorescent emitting layer. The device structure of the phosphorescent blue OLEDs consisted of the following: Glass/indium tin oxide (ITO, 70 nm)/ ReO_3 (4 wt%) doped N,N'-dicarbazolyl-3,5-benzene (mCP, 30 nm)/mCP (10 nm)/mCPPO1: iridium complexes (30 nm, 10 wt%)/ diphenylphosphine oxide-4-(triphenylsilyl)phenyl (TSPO1, 10 nm)/Rb_2CO_3 (8 wt%)-doped mCP (30 nm)/Al (100 nm). The hole injection layer (HIL) was doped with a p-type dopant, ReO_3 [rhenium(VI) oxide][28-30] and the electron injection layer (EIL) was doped with an n-type dopant, Rb_2CO_3,[31-33] to facilitate efficient hole and electron injection from the electrodes. The mCP and TSPO1 layers functioned as the hole- and electron-transporting layers, respectively. Compound mCPPO1 was chosen as the host material owing to its high triplet energy and the balance of electron and hole mobilities that if offers.[19] The LUMO level of mCPPO1 was 0.24 eV lower than that of mCP, and its HOMO level was 0.59 eV higher than that of TSPO1, leading to effective exciton blocking. Moreover, the triplet energy levels of all the constituent materials were higher than those of the iridium complexes. Therefore, it was expected that charge carrier and triplet exciton would be confined within the emitting material layer (EML).

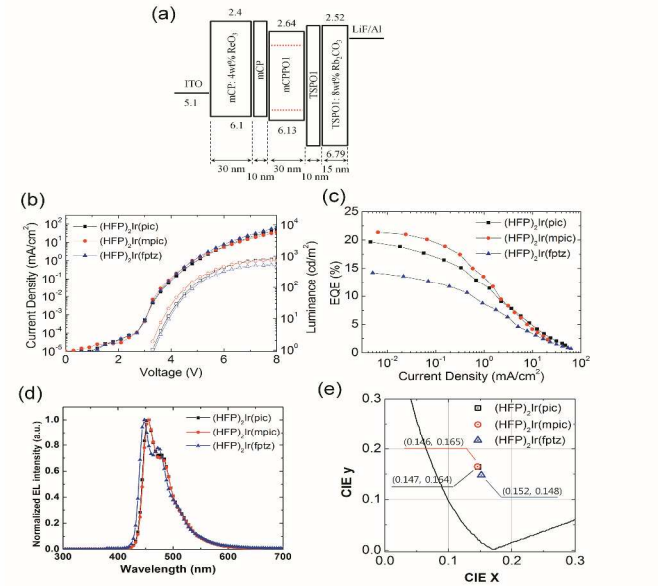

Figure 3. (a) Device structure, energy level diagrams of the OLEDs (b) Current density−voltage−luminance curves, (c) quantum efficiencies versus current density curves, and (d) normalized EL spectra of the different phosphorescent blue OLEDs at 5 mA/cm^2. (e) Comparison of the CIE coordinates of the EL from the OLEDs.

The current density-voltage-luminance (J-V-L) characteristics of the OLEDs are shown in Figure 3 (b). The J-V characteristics of all the three devices were similar because of their similar structure, which varied only by the dopants used in each. In contrast, the devices based on $(HFP)_2Ir(pic)$ and $(HFP)_2Ir(mpic)$ showed higher maximum luminance than did $(HFP)_2Ir(fptz)$. The external quantum efficiencies (EQEs) of the OLEDs are shown in Figure 3 (c). The device with $(HFP)_2Ir(mpic)$ showed the highest EQE among the three devices followed by $(HFP)_2Ir(pic)$ and $(HFP)_2Ir(fptz)$, an observation consistent with the PLQYs of the dopants. The maximum EQEs were 19.7%, 21.4% and 14.2% for the devices containing $(HFP)_2Ir(pic)$, $(HFP)_2Ir(mpic)$, and $(HFP)_2Ir(fptz)$, respectively. The power efficiencies of the devices were 22.3, 25.9 and 14.5 lm/W for the devices containing $(HFP)_2Ir(pic)$, $(HFP)_2Ir(mpic)$, and $(HFP)_2Ir(fptz)$, respectively. The performances of the three OLEDs are summarized in Table S2. The electroluminescence (EL) spectra of the three devices at 5 mA/cm^2 are shown in Figure 3 (d). The emission peaks (EL_{max}) of the OLEDs based on $(HFP)_2Ir(pic)$ and $(HFP)_2Ir(mpic)$, were both located at 452 nm, while that of the device based on $(HFP)_2Ir(fptz)$, was located at 447 nm. The values of the full width at half maximum for the emission of all three devices were less than 50 nm. Owing to the spectral purities of the emissions from the OLEDs, the CIE

coordinates (x,y) of the devices containing $(HFP)_2Ir(pic)$, $(HFP)_2Ir(mpic)$, and $(HFP)_2Ir(fptz)$, at 100 cd/m^2 were (0.147, 0.164), (0.146, 0.165), and (0.152, 0.148), respectively.

Conclusions

Three new deep-blue iridium(III) complexes, (HFP)2Ir(pic), $(HFP)_2Ir(mpic)$, and $(HFP)_2Ir(fptz)$, consisting of a heptafluoropropyl substituted at 2',4''-difluororphenyl-3-methylpyridine as the main ligand and a picolinate, a picolinate with 3- methylpyridine or a trifluoromethylated triazole as the ancillary ligand, were successfully synthesized and characterized. We demonstrated the strong electron-withdwawing heptafluoropropyl groups more affect the HOMO level than that of LUMO level, as determined by TD-DFT calculations. As a results, these iridium complexes exhibited wide band gaps with high PL QYs. Phosphorescent OLEDs based on $(HFP)_2Ir(pic)$, $(HFP)_2Ir(mpic)$, and $(HFP)_2Ir(fptz)$ exhibited high maximum EQEs of 19.7%, 21.4% and 14.2% and CIE coordinates of (0.147, 0.164), (0.146, 0.165) and (0.152, 0.148), respectively. These CIE coordinates represent some of the deepest blue emissions ever achieved from phosphorescent OLEDs with considerably high EQEs.

Acknowledgements

This work was supported by the industrial strategic technology development program [10035225, Development of core technology for high performance AMOLED on plastic] funded by MKE/KEIT

Notes and references

1 D. Tanaka, H. Sasabe, Y.-J. Li, S.-J. Su, T. Takeda, and J. Kido, Jpn. *J. Appl. Phys*. 2007**, 46,** 1.
2 M. G. Helander, Z. B. Wang, J. Qiu, M. T. Greiner, D. P. P. Puzzo, Z. W. Liu, Z. H. Lu, *Science*. 2011, **332**, 944.
3 Y.-S. Park, S. Lee, K.-H. Kim, S.-Y. Kim, J.-H. Lee, J.-J. Kim, *Adv. Funct. Mater*. 2013, **23**, 4914.
4 S.-Y. Kim, W.-I. Jeong, C. Mayr, Y.-S. Park, K.-H. Kim, J.-H. Lee, C.-K. Moon, W. Brütting, J.-J. Kim, *Adv. Funct. Mater*. 2013, **23**, 3896.
5 S. Lee, K.-H. Kim, D. Limbach, Y.-S. Park, J.-J. Kim, *Adv. Funct. Mater*. 2013, **23**, 4105.
6 L. Xiao, S.-J. Su, Y. Agata, H. Lan, J. Kido, *Adv. Mater*. 2009, **21**, 1271.
7 S.-J. Su, T. Chiba, T. Takeda, J. Kido, *Adv. Mater*. 2008, **20**, 2125.
8 H. Sasabe, E. Gonmori, T. Chiba, Y.-J. Li, D. Tanaka, S.-J. Su, T. Takeda ,Y.-J. Pu ,K. Nakayama, J. Kido, *Chem. Mater*. 2008, **20**, 5951.
9 N. Chopra, J. Lee, Y. Zheng, S.-H. Eom, J. Xue, F. So, *Appl. Phys. Lett*. 2008, **93**, 143307.
10 J.-K. Bin, N.-S. Cho, J.-I. Hong, *Adv. Mater*. 2012, **24**, 2911.
11 C. Fan, Y. Li, C. Yang, H. Wu, J. Qin, Y. Cao, *Chem. Mater.* 2012, **24**, 4581-4587.
12 C. Fan, L. Zhu, B. Jiang, D. Ma, J. Qin, C. Yang, *Org. Electron.* 2013, **14**, 3163-3171.
13 C.-L. Ho, W.-Y. Wong, *New J.Chem*. 2013, **37**, 1665-1683
14 C.-L. Ho, H. Li, W.-Y. Wong, *New J.Organomet. Chem.* 2014, **751**, 261
15 R. J. Holmes, S. R. Forrest, T. Sajoto, A. Tamayo, P. I. Djurovich, M. E. Thompson, J. Brooks, Y.-J. Tung, B. W. D'Andrade, M. S. Weaver, R. C. Kwong, and J. J. Brown, *Appl. Phys. Lett*. 2005, **87**, 243507
16 C.-H. Yang, Y.-M. Cheng, Y. Chi, C.-J. Hsu, F.-C. Fang, K.-T. Wong, P.-T. Chou, C.-H. Chang, M.-H. Tsai, and C.-C. Wu, *Angew. Chem. Int. Ed.* 2007, **46**, 2418
17 Y.-C. Chiu, J.-Y. Hung, Y. Chi, C.-C. Chen, C.-H. Chang, C.-C. Wu, Y.-M. Cheng, Y.-C. Yu, G.-H. Lee, and P.-T. Chou, *Adv. Mater*. 2009, **21**, 2221
18 S. O. Jeon, K. S. Yook, C. W. Joo, and J.Y. Lee, *Adv. Mater*. 2010, **22**, 1872.
19 S. O. Jeon, K. S. Yook, C. W. Joo, and J. Y. Lee , *Adv. Mater*. 2011, **23**, 1436.
20 P. J. J. Hay, *Phys. Chem. A*, 2002, **06,** 1634.
21 S. O. Jung, Y. Kang, H. S. Kim, Y. H. Kim, C. L. Lee, J.-J. Kim, S. K. Kwon, *Eur. J. Inorg. Chem*. 2004, **17**, 3415.
22 S. Lee, S.-O. Kim, H. Shin, H.-J. Yun, K. Yang, S.-K. Kwon, J.-J. Kim, and Y.-H. Kim, *J. Am. Chem. Soc*. 2013, **135**, 14321.
23 V. V. Grushin, N. Herron, D. D. LeCloux, W. J. Marshall, V. A. Petrov, Y. Wang, *Chem. Commun*. 2001, 1494. ;DOI: 10.1039/B103490C
24 S.-O. Kim, Q. Zhao, K. Thangaraju, J.-J. Kim, Y.-H. Kim, S.-K. Kwon, *Dyes Pigm*. 2011, **90**, 139.
25 P. J. Hay, W. R. Wadt, *J. Chem. Phys.* 1985, **82**, 299.
26 M. E. Casida, C. Jamorski, K. C. Casida, D. R. Salahub, *J. Chem. Phys*. 1998, **108**, 4439.
27 H.-J. Seo, K.-M. Yoo, M. Song, J.-S. Park, S.-H. Jin, Y.-I. Kim, Y.-I. Kim, J.-J. Kim, *Org. Electron.* 2010, **11**, 564.
28 D.-S. Leem, H.-D. Park, J.-W. Kang, J.-H. Lee, J. W. Kim, J.-J. Kim, *Appl. Phys. Lett*. 2007, **91,** 011113
29 J.-H. Lee, D.-S. Leem, H.-J. Kim, J.-J. Kim, *Appl. Phys. Lett*. 2009, **94**, 123306.
30 J.-H. Lee, D.-S. Leem, J.-J. Kim, *Org. Electron*. 2010, **11**, 486.
31 D.-S. Leem, S.-Y. Kim, J.-J. Kim, M.-H. Chen, C.-I. Wu, *ECS Solid State Lett*. 2009, **12**, J8.
32 M.-H. Chen, Y.-H. Chen, C.-T. Lin, G.-R. Lee, C.-I Wu, D.-S. Leem, J.-J. Kim, T.-W. Pi, *J. Appl. Phys*. 2009, **105**, 113714.
33 S. Lee, J.-H. Lee, J.-H. Lee, J.-J. Kim, *Adv. Funct. Mater*. 2011, **21**, 855.

